

High molecular weight polyacrylamide nanoparticles prepared by inverse emulsion polymerization: reaction conditions-properties relationships

Y. Tamsilian¹ · A. Ramazani S.A.^{1,2} · M. Shaban¹ · Sh. Ayatollahi^{1,2} · R. Tomovska^{3,4}

Received: 12 June 2015 / Revised: 28 September 2015 / Accepted: 23 November 2015 / Published online: 11 December 2015
© Springer-Verlag Berlin Heidelberg 2016

Abstract High molecular weight polyacrylamide (PAM) nanoparticle dispersions are products with wide application possibilities, the most important of which is in petroleum industry such as drilling fluid and flooding agent in enhanced oil recovery. For that aim, it is necessary to achieve complete control of the final dispersion and polymer properties during the synthesis step. In this work, PAMs were synthesized by inverse emulsion polymerization of aqueous acrylamide solution in cyclohexane in the presence of emulsifier mixture of Span 20 and Span 80. We present a comprehensive study of the effects of variation of all important reaction conditions (agitation rate, reaction time and temperature, initiator type and concentration, emulsifier HLB ratio and its concentration, and water to oil ratio) on final monomer conversion, reaction kinetics, polymer intrinsic viscosity and molecular weight, particle size and distribution, and colloidal stability. Finally,

the relationships between the reaction conditions and the polymer properties were developed, which allowed determination of the ranges of variation of reaction conditions for optimal PAM properties for the oil industry applications: high molecular weight and intrinsic viscosity, nanosized polymer particles with narrow particle size distribution, and improved colloidal stability of the final dispersions.

Keywords Polyacrylamide nanoparticles · Inverse emulsion polymerization · Molecular weight · Particle size · Second virial coefficient · Reaction kinetics

Introduction

Water-soluble polymers, such as polyacrylamide (PAM) and its derivatives, are the most important synthetic water-soluble polymers because of their numerous applications. Acrylamide-based polymers are widely used as commercial products, particularly in coagulants and flocculants during wastewater treatment applications [1], drag reduction agents [2], polymeric additive in drilling fluids [3], displacing fluids in the enhanced oil recovery (EOR) [4], additives in paper making [5], and drug-delivery agents [6–9].

Water in oil (W/O) or inverse emulsion polymerization is an ideal and the most investigated method for preparation of water-soluble polymer nanoparticles with high molecular weight and low viscosity [10–22]. It has been demonstrated that the initiator type and amount, and emulsifier type and amount are important parameters that affect the kinetics of inverse emulsion polymerization [10–14]. Large range of different solvents have been used as continuous phase, reaction loci, and the reservoir of monomer in the inverse emulsion polymerization of acrylamide (AM), such as toluene [15–18], heptane [16], isooctane [13], or xylene [19]. The

Electronic supplementary material The online version of this article (doi:10.1007/s00396-015-3803-5) contains supplementary material, which is available to authorized users.

✉ A. Ramazani S.A.
ramazani@sharif.edu

✉ R. Tomovska
radmila.tomovska@ehu.es

¹ Institute for Nanoscience and Nanotechnology (INST), Sharif University of Technology, P.O. Box 11155-8639, Tehran, Iran

² Chemical and Petroleum Engineering Department, Sharif University of Technology, P.O. Box 11155-9465, Tehran, Iran

³ Institute for Polymer Material POLYMAT, Universidad del País Vasco/Euskal Herriko Unibertsitatea (UPV-EHU), Joxe Mari Korta Center, 20018 Donostia-San Sebastian, Spain

⁴ IKERBASQUE, Basque Foundation for Science, Maria Diaz de Haro 3, Bilbao 48013, Spain

results indicated that the molecular weight, particle size, and its distribution of the final product depend on the type of continuous phase, which seems to influence kinetics of the process importantly. Only few studies have been performed to determine the effect of process parameters, such as hydrophilic-lipophilic balance of the emulsifier used (HLB) [19, 20], emulsifier type and concentration [19, 21], initiator type and concentration [19, 21, 22], reaction temperature [19], and rate of agitation [19] on the kinetics inverse emulsion polymerization and the final PAM properties.

It was showed that more stable inverse emulsions were obtained using the HLB value of emulsifier system at or higher than 5.6, wherein the conversion rate, molecular weight, and particle size were independent on HLB value variations [19, 22]. On the other hand, at constant HLB value, the particle size, its distribution, and polymerization rate were decreased as the emulsifier concentration increased [21, 22], whereas molecular weight of the final polymer increased by increasing emulsifier concentration up to certain critical concentration. Although polymerization rate was affected by emulsifier concentration, final conversions were similar for reactions performed at various emulsifier concentrations [19]. Increasing the rate of agitation during polymerization process induced drop of the average size of polymer particles and their distributions, resulting from a balance between coalescence and dispersion of the emulsion droplets [19, 20, 22]. Concerning the initiator type, 2,2'-azobis(isobutyronitrile) (AIBN) oil-soluble and water-soluble potassium persulfate (KPS) initiators have been compared for inverse emulsion polymerization of AM, and very similar kinetic behavior was observed [21], discussed in terms of similar hydrophobicity, diffusivity through the polymerization system, and partitioning between the phases of the formed radicals. In the case of water-soluble initiator (KPS), it was noticed that by augmentation of its content, final conversion and particle size and distribution decreased while the initial polymerization rate increased [19, 20].

It is clear that the reaction conditions influence significantly the final PAM properties and the properties of its nanoparticles dispersions. Even though, up to our best knowledge, there are no systematic studies for establishment of thorough relationships between all the important reaction conditions and the final application properties of the PAMs. This is especially true for the PAM dispersions colloidal stability that can be significantly influenced by tiny changes in the formulation. In the present study, via design of experiments, we have performed thorough investigation of the effect of the most important reaction conditions, including agitation rate, reaction temperature, initiator type, and concentration, HLB value of the emulsifier system and its concentration, polymerization time, and water to oil phase (W/O) ratio in the inverse emulsion polymerization of AM on the reaction kinetics of PAM, important PAM properties, and properties of the nanoparticle

dispersions (viscosity-average molecular weight, intrinsic viscosity, particle size and its distribution, second virial coefficient as stability index). Besides others, the variation in dispersion colloidal stability has been investigated in correlation with the other important properties, toward their optimization for application in petroleum industry as drilling fluids and oil recovery enhancers of the final properties (high molecular weight PAM nanoparticles with high intrinsic viscosity, narrow particle size distributions, and very good particle interaction strength and colloidal stability).

Materials and methods

Materials

Acrylamide (AM, $\geq 99\%$), ammonium persulfate (APS, $\geq 99.9\%$), 2,2'-Azobis(isobutyronitrile) (AIBN, $\geq 98.9\%$), and cyclohexane ($\geq 99.9\%$) were used as received from ChemLab company. The sorbitan monooleate emulsifiers including Span 80 (Merck, HLB value = 4.3), Span 20 (Merck, HLB value = 8.6), and a mixture of them were used without further purification. Doubly distilled water used for the preparation of emulsion was deprived of oxygen by heating to boiling point and cooling under a stream of nitrogen.

Recipe and polymerization procedure

The inverse emulsion polymerization of AM was carried out in a 250-mL five-neck flask equipped with a mechanical stirrer, thermometer, submicron dropping injector for initiator ingredient, and nitrogen gas inlet and outlet. First, cyclohexane as an organic solvent and emulsifier (Span 20, Span 80, and a mixture of them) were mixed by the homogenizer (Ultra Turrax, IKA works, USA) into a beaker (~20,000 rpm, 10 min). After complete dissolution of the dispersion stabilizer in the solvent for 10 min, AM monomer dissolved in deionized water was slowly dripped into the beaker by submicron dropping injector within 15 min to form inverse water in oil (W/O) emulsion under severe mixing (~24,000 rpm, 15 min). The obtained milky emulsion was then transferred to the flask, placed in the water bath at the constant temperature of 30 °C. Then, temperature and stirrer speed were set as shown later. Initiator solution (APS or AIBN) was then charged into the reaction mixture. The polymerization process was performed for different initiator concentration and type, agitation rate, emulsifier concentration and type, reaction time and temperature, and W/O ratio.

In this study, the effect of seven variables as input factors such as agitation rate, reaction time and temperature, initiator concentration and type, emulsifier concentration, W/O ratio, and hydrophilic-lipophilic balance value of the emulsifier system on six responses including viscosity-average molecular

weight (M_w), particle size (d) and its distribution (PSD), intrinsic viscosity ($[\eta]$), second virial coefficient (A_2), and monomer conversion (X) of PAM nanoparticles were investigated. To study the effect of initiator type on the reaction kinetics, two different initiators with the same molar concentrations were used in the inverse emulsion polymerization of AM. AIBN was used as hydrophobic initiator, whereas APS as a hydrophilic initiator. To show the quantitative effects, a set of experiments was designed, as shown in Table 1, where AM denotes acrylamide, CH is cyclohexane, C_E is emulsifier concentration, C_I is initiator concentration, W/O ratio is ratio of water phase to oil phase, HLB is hydrophilic-lipophilic balance, t_r is polymerization time, T is reaction temperature, and N is agitation rate.

It is worthwhile noting that run 1, 3, 5, 6, 8, 12, and 15 (Table 1) were repeated to check the reproducibility of the results. The repeated experiments showed that the experimental errors were in the range of $\pm 0.2\%$ for monomer conversion, $\pm 1\%$ for intrinsic viscosity and molecular weight, $\pm 1.5\%$ for particle size and distribution, and $\pm 3\%$ for second virial coefficient.

Characterizations

Monomer conversion measurement

To measure conversion of AM as a function of time, 10 g of dispersion (m_1) was withdrawn from the reaction vessel at various time intervals. Hydroquinone aqueous solution (0.5 wt%) was added to each sample in order to stop the polymerization progress. Samples were precipitated with excess amount of acetone (1:6) and the obtained precipitates were dried by freeze dryer (Model: FD-10; Pishtaz Engineering Co.) at $-50\text{ }^\circ\text{C}$ for 48 h to reach constant weights (m_2). Finally, conversion of PAM nanoparticles was calculated by Eq. 1.

$$x\% = \frac{m_2 - \text{Hydroquinone weight}}{m_1 \times \frac{\text{Initial Monomer Weight}}{\text{All ingredients weight in recipe}}} \times 100\% \quad (1)$$

Emulsion particle size and distribution

Z-average diameter of PAM nanoparticles and particle size distribution were measured by Malvern Zetasizer Nano Series dynamic light scattering using a laser as light source with wavelength of 640 nm under scattering angle of 90° at ambient temperature ($25\text{ }^\circ\text{C}$) immediately after injecting the emulsions into 10 wt% solution of Span 80 in cyclohexane under vigorous mixing ($\sim 10,000$ rpm). In particle size measurements by field emission scanning electron microscopy (FE-

SEM, Model TESCAN MIRA3LMU, Cambridge Instrument Co.), one drop of final emulsion without any treatment was placed on the sample holder and then spin coated (5000 rpm, 40 s) for removing the water. It should be noted that the Z-average (cumulants mean) used in dynamic light scattering measurements is an intensity-based calculated value of particles size and the best value to report for particles size in respect to even small changes in the sample, e.g., the presence of a small proportion of aggregates.

Determination of intrinsic viscosity and molecular weight

Molecular weights of the final polymers were determined by Ubbelohde capillary viscometry method using the Mark-Houwink equation (Eq. 2) for PAM dissolved in water at $25\text{ }^\circ\text{C}$ [23].

$$[\eta]_{\text{intrinsic}} \left(\frac{\text{mL}}{\text{g}} \right) = 6.31 \times 10^{-3} M_w^{0.8} \left(\frac{\text{g}}{\text{mol}} \right) \quad (2)$$

A portion of each final emulsion was precipitated by an excess amount of acetone (1:6) and washed several times by acetone. Precipitates were then dried at $60\text{ }^\circ\text{C}$ for 48 h. Two hundred milligrams of the purified polymer powder was dissolved in 100 mL deionized water under stirring. The obtained solution (0.2 g of polymer in 100 mL of solution) was diluted to prepare concentrations of 0.16, 0.12, 0.08, and 0.04 g of polymer in 100 mL deionized water. Viscosity of each solution was measured three times by a capillary viscometer (constant factor = $0.01024\text{ mm}^2/\text{s}$). The intrinsic viscosity, $[\eta]$, was determined from intercept value of a linear regression of relationship between the specific viscosity and polymer concentration. In addition, molecular weights of the final polymers were determined by DLS method (Debye plot) using the following section for polyacrylamide aqueous solutions.

Determination of second virial coefficient

Debye plot, which is a linear fit of KC/R_θ vs. concentration (Eq. 3), where the intercept is equal to the inverse of the molecular weight and the slope is twice the second virial coefficient.

$$\frac{KC}{R_\theta} = \frac{1}{M_w} + 2A_2C \quad (3)$$

In above equation, K is an optical constant, C is the particle concentration, R_θ is the Rayleigh ratio of scattered to incident light intensity, M is the weight average molecular weight, A_2 is the second virial coefficient, and $1/P_{(\theta)}$ embodies the angular dependence of the sample scattering intensity.

Data collection and calculations for PAM nanoparticle solutions (0.002, 0.004, 0.006 g/mL) were managed using the molecular weight function in the DTS software for the

Table 1 Design of experiments to synthesize PAM nanoparticles

Run	Initiator	AM, wbt%	Water, wbt%	CH, wbt%	C_E , wbt%	C_I , mM	W/O ratio	HLB	t_p , min	T , °C	N , rpm
1	APS	3.9	5.1	89.8	1.2	7.27E-04	0.1	6.5	120	60	500
2	APS	5.7	11.3	81.9	1.1	7.51E-04	0.2	6.5	120	60	500
3	APS	7.0	16.0	76.0	1.0	7.69E-04	0.3	6.5	120	60	500
4	APS	15.2	34.8	49.3	0.7	8.88E-04	0.5	6.5	120	60	500
3'	APS	7.0	16.0	76.0	1.0	7.69E-04	0.3	6.5	20	60	500
3''	APS	7.0	16.0	76.0	1.0	7.69E-04	0.3	6.5	200	60	500
5	APS	7.0	16.0	76.0	1.0	7.69E-04	0.3	6.5	120	40	500
6	APS	7.0	16.0	76.0	1.0	7.69E-04	0.3	6.5	120	50	500
7	AIBN	7.0	16.0	76.0	1.0	7.69E-04	0.3	6.5	200	60	500
8	APS	7.0	16.0	76.0	1.0	3.85E-03	0.3	6.5	120	60	500
9	APS	7.0	16.0	76.0	1.0	1.15E-02	0.3	6.5	120	60	500
10	APS	7.0	16.0	76.0	1.0	7.69E-04	0.3	6.5	120	60	200
11	APS	7.0	16.0	76.0	1.0	7.69E-04	0.3	6.5	120	60	800
12	APS	7.0	16.0	76.0	1.0	7.69E-04	0.3	4.3	120	60	500
13	APS	7.0	16.0	76.0	1.0	7.69E-04	0.3	8.6	120	60	500
14	APS	7.0	16.0	76.9	0.1	7.61E-04	0.3	6.5	120	60	500
15	APS	7.0	16.0	76.5	0.5	7.65E-04	0.3	6.5	120	60	500
16	APS	7.0	16.0	73.5	3.5	7.92E-04	0.3	6.5	120	60	500

wbt weight based on total weight of all ingredients (AM, Water, CH, C_E)

The initiator concentration is millimolar based on water plus cyclohexane volumes

Zetasizer Nano system, which compiles the static intensity measurements, generates a standard Debye, and then calculates the molecular weight and second virial coefficient. The second virial coefficient represents particle interaction strength and has been correlated with sample solubility [24]. The negative value measured in a sample shown in Debye plot indicates that the polymer has a preference toward aggregation as opposed to solvation.

Results and discussion

When the AM inverse emulsions were prepared by mild mixing of the phases using only mechanical stirrer with max agitation rate of 2000 rpm, emulsion color changed from yellow to brown, although the water/AM solution was injected to the colorless organic solution. The color change reveals an unstable emulsion, which was separated into two phases after ceasing of mixing (Fig. 1a). However, when a high-speed homogenizer (max agitation rate of 24,000 rpm) and a mechanical stirrer were subsequently applied to generate a vigorous stirring, milky colored emulsions were obtained with abruptly increased stability (Fig. 1b). In this way, prepared emulsions were stable for several days at a room temperature, which demonstrates that the treatment of water/AM/cyclohexane/emulsifier mixtures using homogenizer produced stable monomer inverse emulsions.

In the following, we present investigation of the effect of various parameters, some of them studied for the first time in inverse emulsion polymerization of AM, on six responses: particle size (d , nm), particle size distribution (PSD), molecular weights measured by DLS (M_w^{DLS}) and capillary viscosity (M_w^{VIS}), intrinsic viscosity ($[\eta]$), second virial coefficient (A_2), and monomer conversion X (percent) (see Tables 2, 3, 4, 5, and 6) as important properties that define the properties of the PAM polymers and their dispersions.

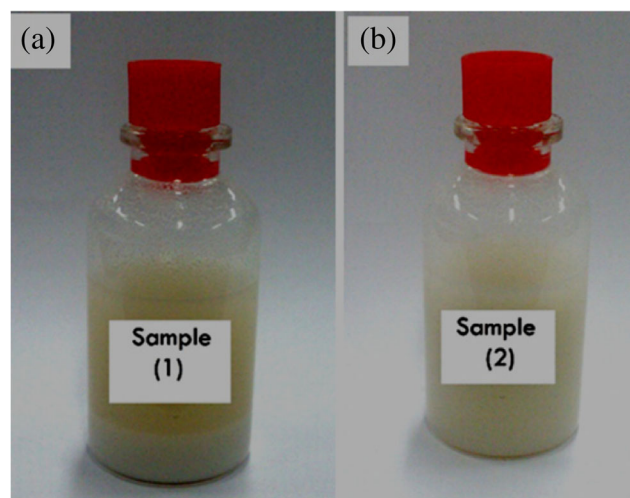


Fig. 1 The prepared monomer emulsions by **a** mechanical mixer (2000 rpm), and **b** homogenizer (24,000 rpm) and mechanical mixer (2,000 rpm)

Table 2 Effect of reaction time and temperature on the inverse emulsion polymerization of AM (other parameters constant, see Table 1)

Run	t_r (min)	T (°C)	Dynamic light scattering technique				Capillary viscometer technique		M_w^{Diff} (%)	X (%)
			d (nm)	PSD	M_w^{DLS} (MDa)	A_2 (mL mol/g ²)	$[\eta]$ (mL/g)	M_w^{VIS} (MDa)		
3'	20	60	60	63–160	0.87	+0.204E-4	343.0	0.84	3.45	67.5
3	120		65	55–179	6.53	+0.670E-4	1674.30	6.02	7.81	98.2
3''	200		63	27–159	6.50	+0.650E-4	1676.0	6.03	7.23	98.9
6	120	50	60	45–190	5.10	+0.684E-4	1469.50	5.11	1.00	82.7
5	120	40	60	50–215	4.00	+0.675E-4	1205.50	3.99	0.25	58.2

It is worth noting that although the polymerization was performed in inverse emulsion, hence it shares some important features of inverse miniemulsion polymerization, such as increased colloidal stability, droplet nucleation, and application of homogenizer for emulsion preparation [25]. Additionally, it has been reported that AM monomer plays a role of co-emulsifier located at the W/O interface, contributing in the increased colloidal stability [26].

Effect of reaction time and temperature

To determine the time required for achieving full AM conversion, in run 3 (Table 2), a portion of emulsion was withdrawn from the reaction vessel at various time intervals: 20 min (run 3'), 120 min (run 3), and 200 min (run 3'') and the six responses were measured. According to the results presented in Table 2, these responses reached a constant value after 120 min, revealing the time needed for almost complete monomer conversion. Thus, polymerization time of 120 min was used in the next runs.

Inverse emulsion polymerization of AM was performed at different reaction temperatures, i.e., 40 (run 5), 50 (run 6), and 60 °C (run 3) presented in Table 2. Effect of reaction temperature on reaction kinetics is presented in Fig. 2. It is clear that polymerization rate increased by raising the reaction temperature, leading to a severe increase in conversion throughout whole reaction time and finally almost full conversion was achieved in 120 min only in the reaction performed at 60 °C. Likely, the observed effect is a result of an increase

in the initiator decomposition rate at higher temperature resulting in faster nucleation.

The average particle diameters and their distributions, as it is shown in Table 2, have not changed significantly, speaking about predominant droplet nucleation, feature characteristic of miniemulsions. It is well known that the radicals desorption rate increases by faster radicals' diffusion at increased temperature (diffusion of monomeric radicals to the particle surface is the rate-limiting step for the radical exit [21]). The higher radical desorption rate of the initiator-derived radicals from the droplet phase (as water-soluble APS initiator was used) will lead to increased molecular weight and intrinsic viscosity of final polymers, owing to the decreased average number of radicals per particle (the estimated value for the investigated system at 60 °C according to [21] is much below 0.5). As a result, under the investigated conditions, the ratio of propagation to termination constant at increased temperature will increase and as well the length of the polymer chains and their intrinsic viscosities (Table 2). Stability of the latex dispersions was not influenced by the reaction temperature, as there is no significant difference between the A_2 coefficients (Table 2).

Effect of water oil ratio

Water to oil ratio (W/O) in inverse emulsion polymerization is an important parameter that can influence the kinetics and subsequently the polymer properties. Despite it, W/O ratio has not been investigated, yet in the present system. In order to determine this effect, the reactions were carried out at W/O

Table 3 Effect of W/O ratio on the inverse emulsion polymerization of AM

Run	W/O ratio	Dynamic light scattering technique				Capillary viscometer technique		M_w^{Diff} (%)	X (%)
		d (nm)	PSD	M_w^{DLS} (MDa)	A_2 (mL mol/g ²)	$[\eta]$ (mL/g)	M_w^{VIS} (MDa)		
1	0.1	–	–	–	–	–	–	–	–
2	0.2	67	45–164	4.55	+0.151E-5	1439.00	4.68	2.86	98.0
3	0.3	65	55–179	6.53	+0.670E-4	1674.30	6.02	7.81	98.2
4	0.5	117	60–195	4.90	+0.128E-6	1519.03	4.60	6.12	96.9

Based on Table 1 with different (AM + water/organic solvent + emulsifier) weight ratios

Table 4 Effect of initiator type and concentration on the properties of the polymer and the nanoparticles dispersions (other reaction conditions presented in Table 1)

Run	Initiator type	C_1 (mM)	Dynamic light scattering technique				Capillary viscometer technique		M_w^{Diff} (%)	X (%)
			d (nm)	PSD	M_w^{DLS} (MDa)	A_2 (mL mol/g ²)	$[\eta]$ (mL/g)	M_w^{VIS} (MDa)		
7	AIBN	7.69E-04	78	55–167	5.60	+0.700E-4	1556.4	5.50	1.78	99.0
3	APS	7.69E-04	63	27–159	6.50	+0.650E-4	1676.0	6.03	7.23	98.9
8	APS	3.85E-03	75	59–165	4.80	+0.590E-4	1390.00	4.77	0.62	95.6
9	APS	1.15E-02	73	64–178	2.59	+0.630E-4	838.00	2.53	2.31	99.0

ratios of 0.1, 0.2, 0.3, and 0.5, keeping the amount of monomer constant, and the six responses were determined and the results are presented in Table 3. It should be noted that the highly unstable inverse emulsion system was obtained at W/O ratio = 0.1 (run 1).

The results presented in Table 3 show that final conversion is not significantly affected by the W/O ratio, as also it is shown in Fig. 3, where the conversion vs. reaction time at different W/O ratios are presented. The polymerization rate is lower for increased W/O ratio, likely due to the fact that at increased W/O ratio the amount of water phase in the inverse emulsion increased at constant emulsifier and monomer concentration, resulting in actual decrease of their concentration in water droplets. On the other hand, this will influence the particle size and distribution of final polymer nanoparticles, as at higher W/O ratio owing to the lower surfactant concentration the formed droplets/particles are prone to coagulation because there is no sufficient amount of surfactant to stabilize them.

Decreased colloidal stability at higher W/O ratios is proved by the value of second virial coefficients (A_2 , Table 3, calculated from the Debye plot presented in Fig. S1 Supporting information), which dropped significantly for the W/O=0.5, indicating increasing droplet-droplet interactions and less stable system.

Particle size distributions, presented in Fig. 4 at different W/O ratios, clearly show this tendency as the contribution of the fraction of small particles decreased with increasing W/O ratio. In the intersections of Fig. 4, available SEM images are presented for illustration of the particle size and distribution.

The intrinsic viscosity and molecular weights increased for the W/O ratio augmentation of 0.2 to 0.3 and then dropped by further increase of W/O ratio to 0.5, which indicates that W/O ratio have significant effect on polymer properties. When W/O ratio is low in the recipe (0.2 and 0.3), the particle size and distributions are relatively similar, and the difference in the molecular weights may be owed to lower monomer concentration in droplets/particles at higher W/O. Further increase in W/O ratio to 0.5 obviously destabilizes the system, which importantly increased the average particle diameter and the average number of radicals per particle, resulting in drop of polymer molecular weights. On the other hand, probability of polymerization in water phase (competition between emulsion and solution polymerizations) increases by the W/O ratio, due to promoted interphase mass transfer. The obtained results show that the considered polymer properties are optimal at W/O=0.3, which was used in the next experiments.

Effect of initiator type and concentration

To study the effect of initiator type on reaction kinetics and polymer characteristics, two different initiator types with the same molar concentrations were used: oil-soluble AIBN and water-soluble APS.

The kinetics of inverse emulsion polymerization of AM for the different initiators used is shown in Fig. 5. It is clear that the reaction rate is higher for the system initiated with APS than for the one initiated with AIBN. However, for both of them, almost full conversions were reached in 120 min. The shape of the kinetic curves indicates that for the system

Table 5 Effect of agitation rate on the inverse emulsion polymerization of AM initiated with APS=7.69E-04 mM, $C_E=1$ wbt% at 60 °C

Run	N (rpm)	Dynamic light scattering technique				Capillary viscometer technique		M_w^{Diff} (%)	X (%)
		d (nm)	PSD	M_w^{DLS} (MDa)	A_2 (mL mol/g ²)	$[\eta]$ (mL/g)	M_w^{VIS} (MDa)		
10	200	138	85–255	6.99	−0.100E-6	1837.01	6.76	3.29	97.4
3	500	65	55–179	6.53	+0.670E-4	1674.30	6.02	7.81	98.2
11	800	73	63–158	5.88	+0.825E-4	1645.03	5.89	0.17	98.0

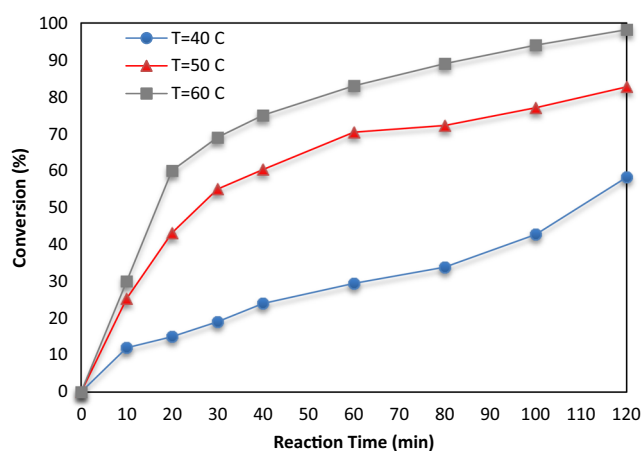
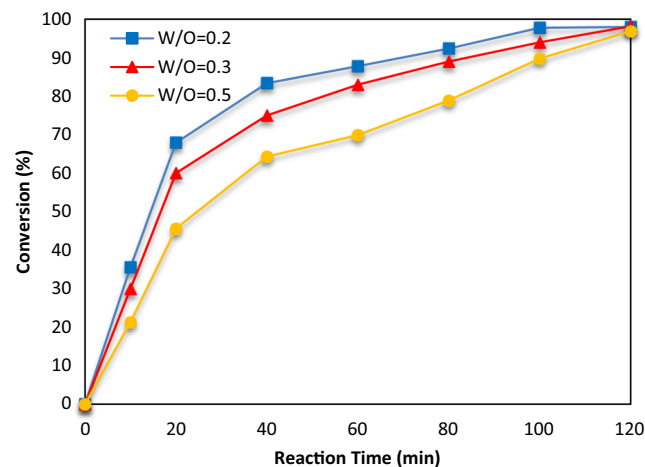
Table 6 Effect of HLB of the emulsifier and its concentration value on the inverse emulsion polymerization of AM

Run	C_E (wbt%)	HLB	Dynamic light scattering technique				Capillary viscometer technique		(%)	X (%)
			d (nm)	PSD	M_w^{DLS} (MDa)	A_2 (mL mol/g ²)	$[\eta]$ (mL/g)	M_w^{VIS} (MDa)		
3	1	6.5	65	55–179	6.53	+0.670E-4	1674.30	6.02	7.81	98.2
12	1	4.3	60	35–150	6.37	+0.100E-5	1650.30	5.90	7.37	97.3
13	1	8.6	80	60–285	6.25	+0.232E-6	1651.00	5.92	5.28	98.4
14	0.1	6.5	–	–	–	–	–	–	–	–
15	0.5	6.5	109	89–252	7.14	+0.333E-6	1900.20	7.05	1.26	99.9
16	3.5	6.5	40	20–130	3.50	+0.164E-4	1128.00	3.67	4.86	87.5

initiated with APS, there are two distinguish regions with different reaction rate, the first one characteristic with higher reaction rate (0–20 min) and the second one with lower reaction rates (20–120 min). On the other hand, the monomer conversion in the reaction initiated by AIBN show kinetic curve that monotonically increased during the whole reaction period. High polymerization rate at lower reaction times in the presence of water-soluble APS initiator can be attributed to the higher concentration of radicals created from APS in the aqueous phase where the monomer is placed [21], which results in fast consumption of APS at the beginning and significant drop in the reaction rate at higher reaction times. Capek [21] suggested that the solubility of radicals and the partitioning of radicals between the oil and water phases is a dominant parameter of the polymerization process. In inverse polymerization of AM initiated with AIBN and APS, they demonstrated that the polymerization process is independent on initiator type, which according to the authors was because of formation of radicals with the similar hydrophobicity, partitioning between W/O phases and similar diffusivity via the reaction system. However, our results show important difference, starting from the kinetic behavior, up to the polymer properties

presented in Table 4. The difference in the behavior probably comes because of difference of the W/O ratio, which was 0.2 in this work and 0.35 in [21]. The different W/O ratio in this system likely alters solubility of radicals and their partitioning between the phases, which finally influences the kinetic behavior and the polymer properties (as shown previously in Table 3).

The effect of initiator type on the properties of the polymer and the nanoparticles dispersions is shown in Table 4 (runs 7 and 3) and in Fig. (S2 Support information). Almost full conversion was achieved in both cases, meaning that the final conversion was not influenced by the initiator type. However, the initiator type has an important effect on d , PSD, $[\eta]$, and M_w . Average particle diameter is larger for AIBN, and the PSD presented in Fig. 6 shows that in the case of APS, there is higher contribution of fraction with lower particle diameters (Fig. 6b). SEM images (presented in the intersection of Fig. 6) confirm this clearly. The lower particle diameter for APS at similar conversions denotes higher number of particles, likely due to faster nucleation. APS and AIBN have similar decomposition rate [21]; however, the lower average particle diameter for APS allows faster radicals desorption from the

**Fig. 2** Variation of monomer conversion with reaction time for different reaction temperatures in the inverse emulsion polymerization of AM (runs 3, 5, and 6)**Fig. 3** Variation of monomer conversion in the inverse emulsion polymerization of AM with reaction time for different W/O ratios (run 3, 15, and 16)

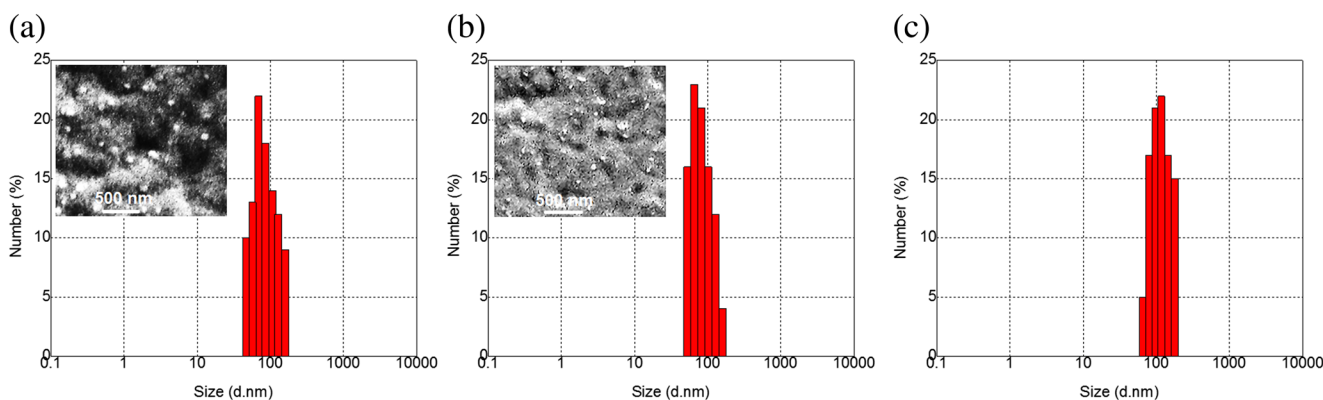


Fig. 4 Particle size distribution of PAM nanoparticles for different W/O ratios (measured by DLS technique; **a** W/O=0.2, **b** W/O=0.3, and **c** W/O=0.5). In the intersection: available SEM images

particles, whereas in the case of AIBN, the radicals derived from initiator in the continuous phase should grow to certain dimension to become more hydrophilic and enter in larger particles. As the radical entry rate increases with increasing particle size [21], this will promote the termination in particles. The faster radical exit from smaller particles in the case of APS resulted in the higher molecular weights, as it is the case (Table 4).

The intrinsic viscosities, determined from Fig. (S3 Supporting information), where the reduced viscosity vs. polymer concentration is presented, as an intersection values at zero concentration, are presented in Table 4 ($[\eta]$ (mL/g)). These values were used to calculate molecular weight of the PAM by Eq. 3 (Table 4, M_w^{VIS}) that are in accordance to M_w^{DLS} . APS-initiated polymerization resulted in higher molecular weight and higher intrinsic viscosity polymers than those initiated with AIBN, likely due to the decreased average number of radicals per particle in the case of APS.

Initiator type has insignificant effect on the A_2 , which means that under investigated conditions the initiator type does not influence the dispersions colloidal stability.

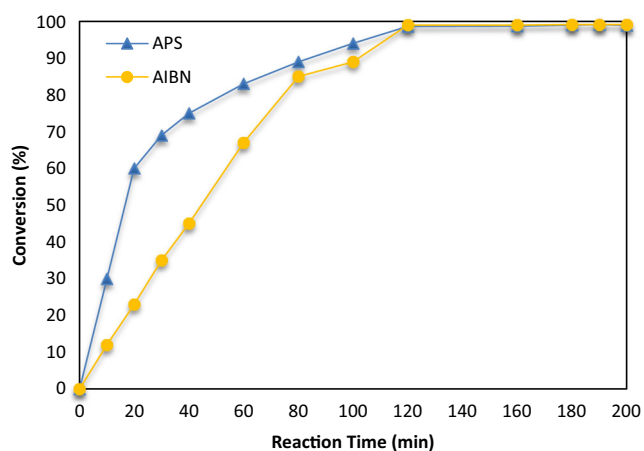


Fig. 5 Variation of monomer conversion in the inverse emulsion polymerization of AM with reaction time for different initiator types (runs 3 and 7)

As the results presented for APS were better with respect to molecular weight and intrinsic viscosity, the effect of initiator concentration was investigated by varying the APS concentrations of 7.69E-04 mM (run 3), 3.85E-03 mM (run 8), and 1.15E-02 mM (run 9). In Table 4, the polymer and dispersion properties are presented and show that particle size is not significantly affected by the initiator concentration, while the intrinsic viscosity (Fig. S4 Supporting information) and molecular weight of final polymer decrease by increasing the initiator concentration due to higher number of initiator-derived radicals within similar size droplet/particles and similar number of particles.

Effect of agitation rate

Role of agitation rate in dispersing of an aqueous monomer solution in the continuous oil phase is unavoidable because the inverse emulsion is not thermodynamically stable system. This section shows the effect of stirring condition on the six responses of the final polymer at three different rates of agitation: 200, 500, and 800 rpm, while the other reaction parameters were maintained constant. The results are summarized in Table 5. According to overall view in Table 5, the agitation rate did not affect the final monomer conversion, whereas other factors including d , PSD, $[\eta]$, M_w , and A_2 are affected, significantly.

The increasing rate of agitation induces drop of average particle diameter, which is clear from Table 5 and Fig. 7 where the PSD and the SEM images of nanoparticles synthesized with different agitation rates are presented. By comparison of Fig. 7a with b and c, it is clear that the fractions of smaller particle sizes (<100 nm) contribute dominantly in the runs obtained at 500 and 800 rpm, whereas at 200 rpm, fractions with 200 nm size appears. SEM image of the sample obtained at 200 rpm (Fig. 7a) shows some agglomerated particles, thus, indicating lack of stability in this sample. It is worth noting that particle agglomerates likely were formed during reaction, as spin coating was used for sample preparation for SEM

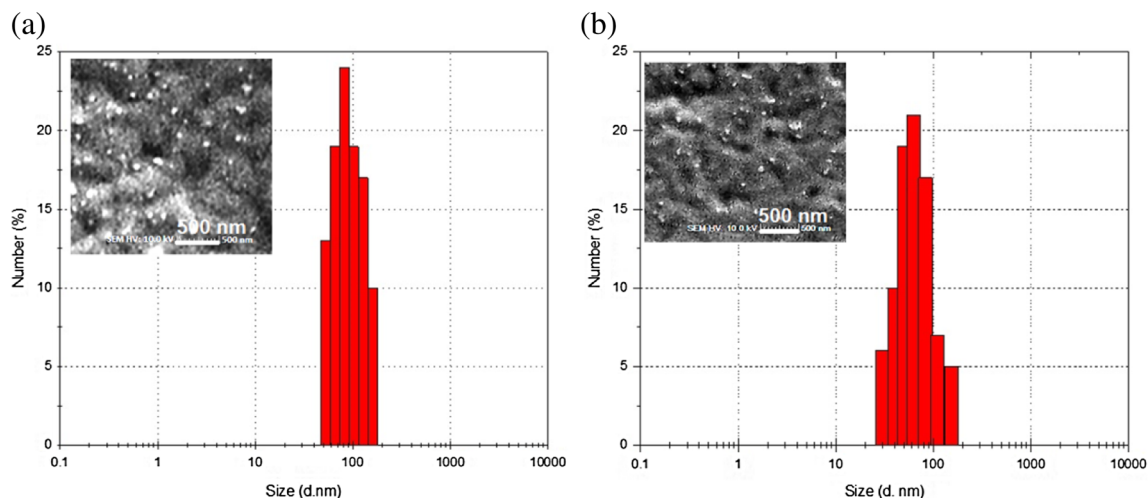


Fig. 6 Particle size distributions and SEM images (in the intersection) of PAM nanoparticles for different initiator types: **a** AIBN and **b** APS

imaging and possibilities that aggregation of particles will occur during sample preparation are minimized. The increased rate of agitation contributes toward significant drop in particle average diameter thereby increase significantly the interfacial area and the number of particles. Thus, one would expect higher molecular weight polymer chains to be formed at higher agitation rate, which is an opposite of what really occurred. The maximum molecular weight of 6.99 MDa (measured by DLS technique) was obtained for an impeller speed of 200 rpm, which descended under higher agitation rate. This effect of agitation rate has been explained in literature, as more oxygen is introduced into reaction loci at higher agitation rates, polymerization rate decreased because of its inhibition effect, and the oxygen contribute in early termination of growing polymer chains, resulting in molecular weight decreased [27, 28].

Debye plot of PAM nanoparticles obtained under different agitation rates, measured by DLS technique (Fig. S5 Supporting information), shows that second virial coefficient as stability parameter of nanoparticles increased by increasing the stirrer rate. As the other parameters during the reactions

were constant, one can suppose that the difference in the values of second virial coefficients comes only from the different size distributions in the dispersions. The highest positive value measured for agitation rate of 800 rpm indicates that the polymer has a preference toward the solvent, whereas the negative value measured for the final polymer particles obtained at 200 rpm represents that particles prefer contact between them resulting in self-sample instability.

Therefore, 500 rpm is found to be the most appropriate agitation rate that brings sufficient colloidal stability to the AM inverse emulsions and the PAM latexes afterward (Fig. S5 Supporting information).

Effect of HLB value and concentration of emulsifier system

As all emulsifiers are amphiphilic molecules and their performance greatly depends on the balance between the hydrophilic and lipophilic parts. Here, the mix of two different surfactants (Span 20 and Span 80) was used, as mentioned, and by changing their ratio, the HLB values were altered. It is well

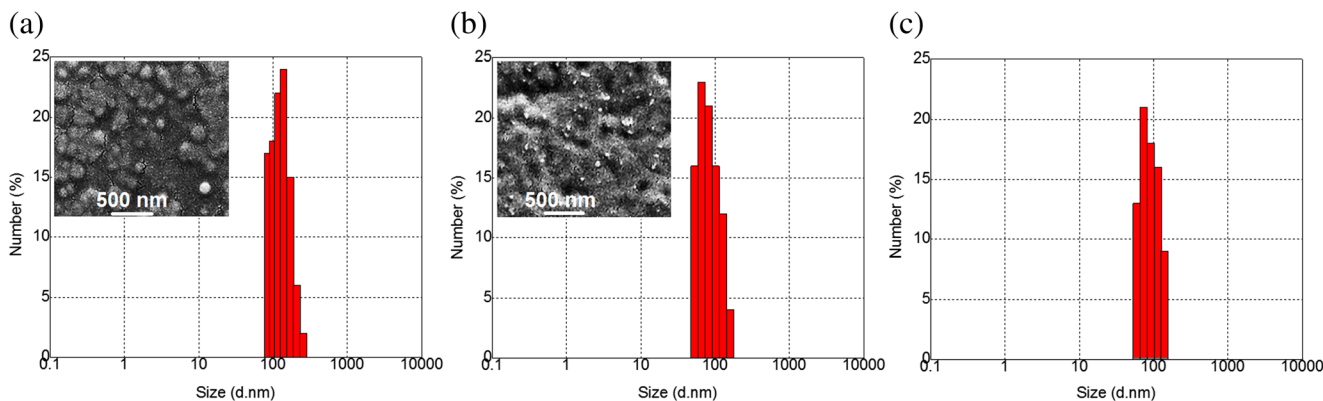


Fig. 7 Particle size distribution of PAM nanoparticles (measured by DLS) and available SEM images (in the intersection) for different agitation rates: **a** $N=200$, **b** $N=500$, and **c** $N=800$ rpm

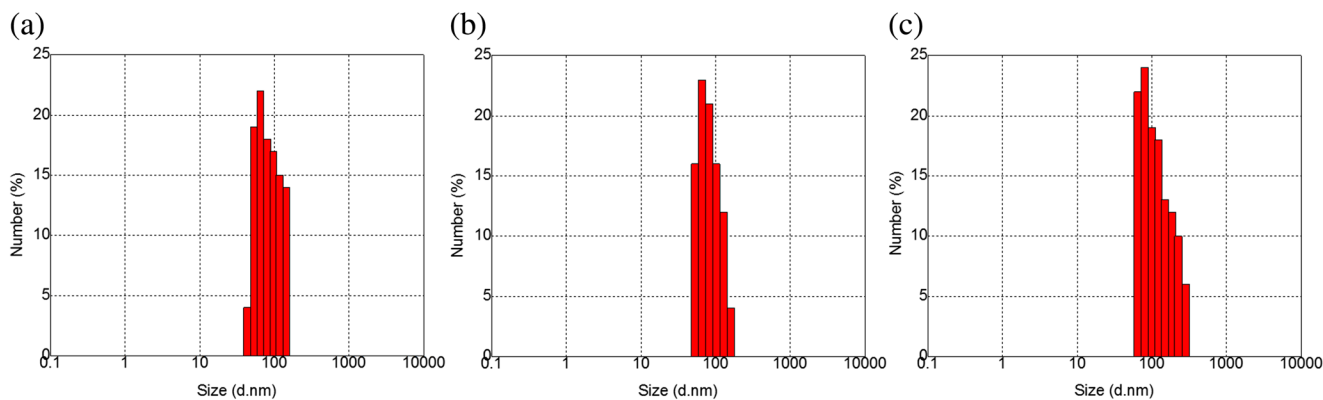


Fig. 8 Particle size distribution of PAM nanoparticles for different HLB values (measured by DLS; **a** HLB=4.3, **b** HLB=6.5, and **c** HLB=8.6)

known that the arrangement of HLB values in the range of 4–6 using two non-ionic emulsifiers, one with high HLB value and another with low HLB value, results in improved colloidal stability of an inverse emulsion system [20, 29]. In the present study, the stable inverse emulsions of aqueous AM solution in cyclohexane was prepared at various HLB of 4.3, 6.5, and 8.6, set at a desirable value (HLB_d) by changing the weight fraction (x) of Span 20 and Span 80 via Eq. 4.

$$x_{\text{span20}} = \frac{(HLB_d - HLB_{\text{Span80}})}{(HLB_{\text{Span20}} - HLB_{\text{Span80}})} \quad (4)$$

HLB value is low when hydrophobic groups are predominant, which is suitable for producing water in oil emulsions. The dependence of the six responses for inverse emulsion polymerization of AM on HLB value is listed in Table 6. It is clear that the monomer conversion as well as the intrinsic viscosity and molecular weight of final polymers are not strongly affected by the HLB value of emulsifier system in the region of 6.5–8.6. However, second virial coefficient, final particle size, and distribution are affected by the HLB value in this region.

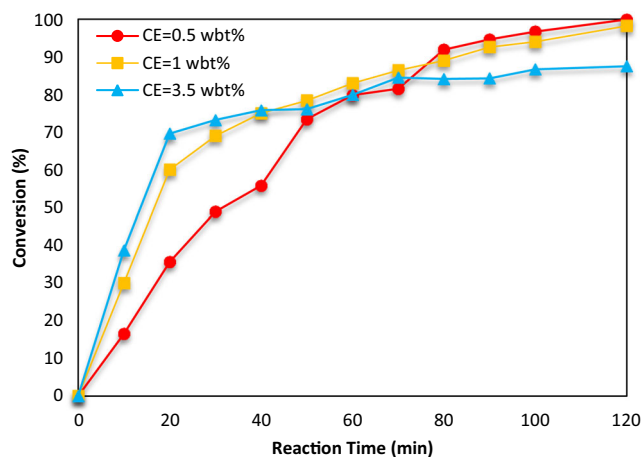


Fig. 9 Variation of monomer conversion in the inverse emulsion polymerization of AM with reaction time for different emulsifier concentrations (runs 3, 15, and 16)

Figure 8 shows PSD of prepared polymer particles at HLB 4.3, 6.5, and 8.6. Regarding these results, average particle size increases by increasing HLB value or by increasing the emulsifier hydrophilicity in the region of 6.5–8.6. It becomes obvious that at higher HLB, the system is less colloidal stable, which is confirmed by the lower second virial coefficient in run 13 (HLB=8.6), calculated from the data presented in the Fig. S6 Supporting information. Apparently, by increased hydrophilicity of the surfactant in the investigated range, the interaction of the nanoparticles with the continuous phase in the inverse miniemulsion decrease and the interparticle interactions are promoted, which resulted in more important contribution of the fractions with higher particle sizes (Fig. 8c). On the other hand, although the particle sizes in runs 3 and 12 are similar, their PSDs are significantly different (see Fig. 8a, b), which give rise to slightly different molecular weights of the polymer chains. It seems that HLB of 6.5 presents an optimal balance of hydrophilic and hydrophobic groups in the emulsifier mixture, as the contribution of the higher particle size fractions is the lowest. As a result, the recipe with HLB value of 6.5 made by mixture of Span 20 (51 wt%) and Span 80 (49 wt%) was selected to be used in the next reactions, because it allows achieving (i) colloidal stable inverse emulsions and (ii) minimum particle size and maximum molecular weight.

Inverse emulsion polymerization of AM was performed at various concentrations of emulsifier under the constant HLB value of 6.5. The kinetic curves are presented in Fig. 9 and the polymer properties in Table 6. It should be noted that the highly unstable inverse emulsion system was obtained at $C_E=0.1$ wbt% (run 14). Figure 9 shows important difference only in the initial reaction period, where the polymerization rate increased with emulsifier concentration. Due to this, for the highest emulsifier content, the full conversion was not achieved, a phenomenon well explained in the literature [21], occurring because of the decreased monomer concentration in the aqueous droplets diluted with surfactants and additionally increased radical desorption rate for smaller particles. As in the present runs, the reaction time

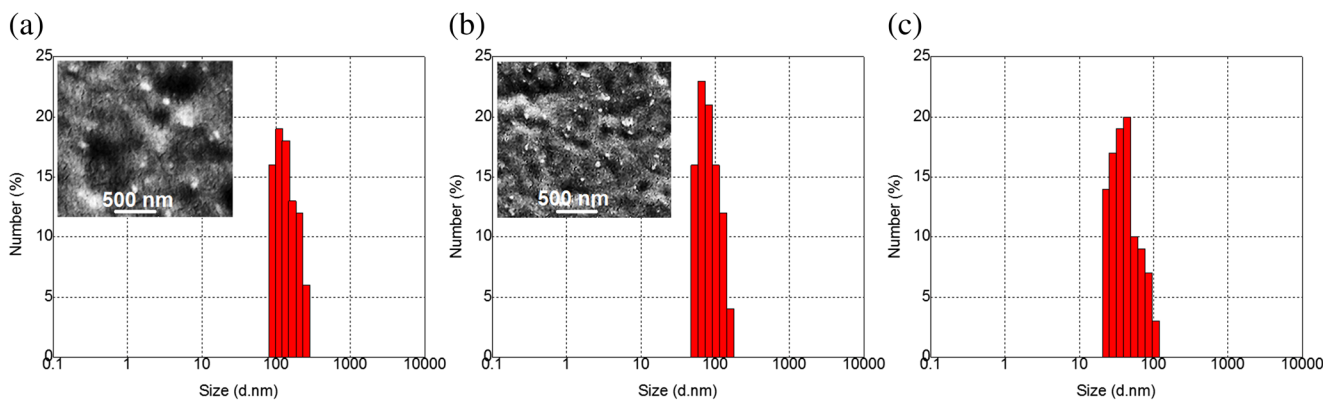


Fig. 10 Particle size distributions and available SEM images (in the intersection) of polyacrylamide nanoparticles for different emulsifier concentrations: **a** $C_E=0.5$, **b** $C_E=1.0$, and **c** $C_E=3.5$ wtb%

was 120 min; obviously, it was not sufficient to achieve higher conversion in this case.

The data presented in Table 6, comparing run 3 ($C_E=0.5$ wtb%), run 15 ($C_E=1$ wtb%), and run 16 ($C_E=3.5$ wtb%), show that emulsifier concentration influences all the investigated polymer and dispersion properties.

PSDs given in Fig. 10 show that particle sizes are reduced by increasing the emulsifier concentration in the investigated range (0.5–3.5 wtb%), whereas second virial coefficients (calculated from the Debye plots presented in Fig. S7 Supporting information) for final polymer nanoparticles initially increases two orders of magnitude by increasing emulsifier concentration. The initial augmentation is likely due to the better coverage of the nanoparticle surface with the emulsifier molecules. Thus, in SEM images of the nanoparticles obtained with 0.5 wtb% (Fig. 10a in the intersection) and 1.0 wtb% (Fig. 10b in the intersection), it can be noted that the lower emulsifier content allows lower nanoparticles coverage, and resulted in some coagulated droplets (decreased second virial coefficient, Table 6), whereas at higher emulsifier contents, the coagulation is dropped significantly. Further augmentation of emulsifier concentration changed the second virial coefficient slightly (fourfold), showing preserved dispersion stability and

decreased particle size and as it is shown in Fig. 10c, the fractions of higher sizes are almost disappeared for 3.5 wtb% emulsifier.

In addition, intrinsic viscosity, and molecular weight of final polymer decreased by increasing the emulsifier concentration (Table 6, Fig. S8 Support information). One could expect the opposite effect because the increased emulsifier content leads to formation of higher number of particles with lower size, thus the average number of radicals per particles decreased. Thus, at such conditions, the terminations would be lower and molecular weights and viscosity higher. However, at high emulsifier concentration, the emulsifier molecules likely act as a chain transfer agent [19] that leads to reduced conversion and lower molecular weights.

Operational conditions-properties relationships

To identify the ranges of operational conditions toward optimal properties of PAM for application of the PAM nanoparticles as drilling fluids and enhanced oil recovery agent in the petroleum industry, for which application it is necessary low particle diameter with narrow size distribution, high molecular weight PAM with high intrinsic viscosity, and very good

Table 7 The ranges of all investigated parameters necessary to produced low particle diameter with narrow size distribution, high molecular weight PAM with high intrinsic viscosity, and very good colloidal stability

Parameter	N (rpm)	HLB	C_1 (mM)	C_E (wtb%)	W/O	t_r (min)	T_r ($^{\circ}C$)
↓ d	500–800	4.3–6.5	7.69E-04	3.5	0.2–0.3	20–120	40–60
↓ PSD	800	4.3–6.5	3.85E-03	3.5	0.2–0.3	20	60
↑ A_2	500–800	6.5	7.69E-04	3.5	0.3	120–200	40–60
↑ M_w	200	4.3–8.6	7.69E-04	0.5	0.3	120–200	60
↑ $[\eta]$	200	4.3–8.6	7.69E-04	0.5	0.3	120–200	60
↑ X	500–800	4.3–8.6	7.69E-04	0.5	0.2–0.3	120–200	60

colloidal stability, in the following we tried to summarize the determined effects and establish the operational conditions-properties relationships. The analyses are performed using only the data with APS water-soluble initiator, as it show in general better desired polymer properties. In summary, the optimal ranges of all investigated parameters are shown in Table 7.

The measurements of PAM nanoparticles average particle diameter indicated that it is affected by agitation rate, HLB value, emulsifier concentration, and W/O ratio. The average particle diameter decreases by increasing emulsifier concentration in the investigated range and by increasing the agitation rate up to 500 rpm after which it remained almost constant. This trend is adverse for increasing of W/O ratio and HLB value. So, in general, PAM particles with average particle sizes generally smaller than 100 nm in diameter are obtained if $C_E > 1$ wt%, $N > 500$ rpm, HLB value = 6.5, and W/O ratio < 0.3 . These ranges are appropriate for narrow particle distributions as well, because particle size distribution decreases by increasing agitation rate, emulsifier concentration, and reaction temperature, whereas it increases by increasing W/O ratio and for HLB values higher than 6.5.

The second virial coefficient, as an indication of colloidal stability of the final dispersions, is affected by agitation rate, HLB value, emulsifier concentration, and W/O ratio. Particle stability increases by increasing the agitation rate and emulsifier concentration in the investigated rang, whereas it decreases by increasing HLB value and W/O ratio. Thus, stable colloidal PAM particles are obtained at HLB=4.3, W/O ratio = 0.3, $C_E > 1$ wt%, and $N > 800$ rpm.

Molecular weight of PAM nanoparticles and their intrinsic viscosities are affected by all investigated factors in which reaction temperature have a positive effect and other parameters adversely influences them. It should be noted that most of the molecular weight values measured with DLS are consistent with the values reported by capillary viscosity technique. The results show that the measured molecular weights by both techniques differ by less than 10 %. The most appropriate limitations for producing high molecular weight polymers are HLB < 6.5 , $C_E < 1$ wt%, $C_1 < 0.1$ wt%, $T_r = 60$ °C, W/O ratio = 0.3, $N < 500$ rpm, and $t_r = 120$ min.

The results presented in Table 7 show that sometime compromise should be established, as for example it is the case for emulsifier concentration, the effect of which adversely influences the molecular weight and particle sizes and distributions.

Conclusion

In this study, a set of reaction conditions have been varied in order to study their effect on the reaction kinetics and monomer conversion, and as well on final polymer and dispersion

properties: colloidal stability (throughout value of second virial coefficient), average particle diameter and particle size distribution of final dispersions, and intrinsic viscosity and molecular weight of the final polymer, determining the relationships between the reaction conditions and the polymer properties. The results showed that the parameters which influence the particle size importantly (such as agitation rate, HLB value, emulsifier concentration, and W/O ratio) significantly affected the reaction kinetics, the distribution of radicals between the phases, and finally the dispersion colloidal stability.

From the determined effects of all the investigated parameters on the final properties, the optimal ranges of the parameters variations were identified toward synthesis of PAM nanoparticles with relatively small average particle diameter (< 100 nm) and narrow distributions, very high molecular weights ($> 4 \times 10^6$ g/mol) and high intrinsic polymer viscosity (> 1200 ml/g). The optimal ranges of the parameters variations to produce the stable colloidal PAM nanoparticles with low particle diameter with narrow size distribution, high molecular weight PAM with high intrinsic viscosity are obtained at $N = 500$ – 800 rpm, HLB=6.5, $C_1 = 7.69E-04$ mM, $C_E = 0.5$ – 3.5 wbt%, W/O ratio = 0.3, $t_r = 120$ – 200 min, and $T_r = 60$ °C. However, for some of the investigated variables, the optimal range remains wide; as it is the case of emulsifier concentration, since it influence adversely the particles size and the molecular weight. In such a case, compromise is needed to be achieved, in accordance to respective application of the produced PAM.

Compliance with ethical standards

Conflict of interest The authors declare that they have no conflict of interest.

References

1. Wada T, Sekiya H, Machi SJ (1976) Synthesis of high molecular weight polyacrylamide flocculants by radiation polymerization. *J Appl Polym Sci* 20:3233–3240
2. Virk PS (1971) Drag reduction in rough pipes. *J Fluid Mech* 45: 225–246
3. Sadeghalvaad M, Sabbaghi S (2015) The effect of the TiO₂/polyacrylamide nanocomposite on water-based drilling fluid properties. *Powder Tech* 272:113–119
4. Wever DAZ, Picchioni F, Broekhuis AA (2011) Polymers for enhanced oil recovery: a paradigm for structure–property relationship in aqueous solution. *Prog in Polym Sci* 36:1558–1628
5. Date JL, Shute JM (1952) Pulp bleaching: principles & practice, Edited by Carlton W. Dence and Douglas W. Reeve. *Tappi* 42:824–826
6. Al-Karawi A, Ahemed Jasim M, AI-Daraji AR (2010) Preparation and using of acrylamide grafted starch as polymer drug carrier. *Carbohydr Polym* 79:769–774

7. Salehi R, Davaran S, Rashidi MR, Entezami AA (2009) Thermosensitive nanoparticles prepared from poly(N-isopropylacrylamide-acrylamide-vinylpyrrolidone) and its blend with poly(lactide-co-glycolide) for efficient drug delivery system. *J Appl Polym Sci* 111:1905–1910
8. Buck S, Pennefather PS, Xue HY, Grant J, Cheng YL, Allen CJ (2004) Engineering lipobeads: properties of the hydrogel core and the lipid bilayer shell. *Biomacro* 5:2230–2237
9. Chaw CS, Chooi KW, Liu XM, Tan CW, Wang L, Yang YY (2004) Thermally responsive core-shell nanoparticles self-assembled from cholesteryl end-capped and grafted polyacrylamides: drug incorporation and in vitro release. *Biomater* 25:4297–4308
10. Lovell PA, El-Aasser MS (1998) Emulsion polymerisation and emulsion polymers. *Polym Int* 45:329–330
11. Ouyang L, Wang L, Schork FJ (2011) Synthesis and nucleation mechanism of inverse emulsion polymerization of acrylamide by RAFT polymerization: a comparative study. *Polym* 52:63–67
12. Hunkeler D (1992) Synthesis and characterization of high molecular weight water-soluble polymers. *Polym Int* 27:23–33
13. Pross A, Platkowski K, Reichert KH (1998) The inverse emulsion polymerization of acrylamide with pentaerythritolmyristate as emulsifier. 1. Experimental studies. *Polym Int* 45:22–26
14. Platkowski K, Pross A, Reichert KH (1998) The inverse emulsion polymerization of acrylamide with pentaerythritolmyristate as emulsifier. 2. Mathematical modelling. *Polym Int* 45:229–238
15. Kurenkov VF, Verizhnikova AS, Myagchenkov VA (1986) Aspects of inversion emulsion polymerization of acrylamide in presence of NaOH and the initiating $K_2S_2O_8$ - $Na_2S_2O_5$ system. *Polym Sci* 28: 543–548
16. Chen LW, Yang W (2004) Photoinitiated, inverse emulsion polymerization of acrylamide: Some mechanistic and kinetic aspects. *J Polym Sci Part A: Polym Chem* 42:846–852
17. Zhung D, Song X, Liang F, Li Z, Liu F (2006) Stability and phase behavior of acrylamide-based emulsions before and after polymerization. *J Phys Chem B* 11:9079–9084
18. Baade W, Reichert KH (1986) Polymerization of acrylamide in dispersion with paraffinic and aromatic liquids as oil phase. *Makromol Chem Rapid Commun* 7:235–241
19. Barari M, Abdollahi M, Hemmati M (2011) Synthesis and characterization of high molecular weight polyacrylamide nanoparticles by inverse-emulsion polymerization. *Iranian Polym J* 20:65–76
20. Graillat C, Pichot C, Guyot A, El-Aasser MS (1986) Inverse emulsion polymerization of acrylamide. I. Contribution to the study of some mechanistic aspects. *J Polym Sci, Part A: Polym Chem* 24: 427–449
21. Capek I (2004) Inverse emulsion polymerization of acrylamide initiated by oil- and water-soluble initiators: effect of emulsifier concentration. *Polym* 36:793–803
22. Blagodatskikh I, Tikhonov V, Ivanova E, Landfester K, Khokhlov A (2006) New approach to the synthesis of polyacrylamide in miniemulsified systems. *Macromol Rapid Commun* 27:1900–1905
23. Scholtan W (1954) Molekulargewichtsbestimmung von polyacrylamid mittels der ultrazentrifuge. *Makromol Chem* 14: 169–178
24. Trabelsi S, Aschi A, Othman T, Gharbi A (2014) Effect of small globular protein on the dynamical behavior of long-chain polyelectrolyte in dilute regime. *Adv Int Polym Tech* 33:3–9
25. Marie E, Rothe R, Antonietti M, Landfester K (2003) Synthesis of polyaniline particles via inverse and direct miniemulsion. *Macromol* 36:3967–3973
26. Candau F (1997) Microemulsion polymerization, In polymeric dispersions: principles and application, J.M. Asua, Ed., NATO ASI. Series E, App Sci 335:127–140, Kluwer academic: Dordrech
27. Krishnan S, Klein A, El-Aasser MS, Sudol ED (2004) Effects of agitation on oxygen inhibition, particle nucleation, reaction rates, and molecular weights in emulsion polymerization of n-butyl methacrylate. *Ind Eng Chem Res* 43:6331–6342
28. Benda D, Snuparek J, Cermak V, (2001), Oxygen inhibition and the influence of pH on the inverse emulsion polymerization of the acrylic monomers, *Euro. Polym. J.*, 1247–1253.
29. Liu X, Xiang S, Yue Y, Su X, Zhang W, Son C, Wang P (2007) Preparation of poly(acrylamide-coacrylic acid) aqueous latex dispersions using anionic polyelectrolyte as stabilizer. *Colloids Surf A: Phys Eng Asp* 311:131–139